J. Fluid Mech. (1977), *vol.* 79, *part* 2, *pp.* 209–229
Printed in Great Britain

A moving fluid interface. Part 2. The removal of the force singularity by a slip flow

By L. M. HOCKING
Department of Mathematics, University College London

(Received 28 April 1976)

If the no-slip condition is used to determine the flow produced when a fluid interface moves along a solid boundary, a non-integrable stress is obtained. In part 1 of this study (Hocking 1976), it was argued that, when allowance was made for the presence of irregularities on the solid boundary, an effective slip coefficient could be found, which might remove the difficulty.

This paper examines the effect of a slip coefficient on the flow in the neighbourhood of the contact line. Particular cases which are solved in detail are liquid–gas interfaces at an arbitrary angle, and normal contact of fluids of arbitrary viscosity. The contribution of the vicinity of the contact line to the force on the boundary is obtained.

The inner region, near the contact line, must be matched with an outer flow, in which the no-slip condition can be applied, in order to obtain the total value of the force on the boundary. This force is determined for the flow of two fluids between parallel plates and in a pipe, with a plane interface. The enhanced resistance produced by the presence of the interface is calculated, and it is shown to be equivalent to an increase in the length of the column of fluid by a small multiple of the pipe radius.

1. Introduction

When the motion in the vicinity of a moving contact line between two fluids and a solid boundary is analysed, the stress on the boundary is found to have a non-integrable singularity. This unrealistic prediction has been discussed by Huh & Scriven (1971) and by Dussan V. & Davis (1974), and it appears to be inescapable if the Navier–Stokes equations and the no-slip boundary condition are assumed to provide an adequately reliable model throughout the flow region. It is, of course, unreasonable to continue to apply a continuum model at distances from the contact line of molecular dimensions. Thus an inner region, close to the contact line, could be examined, where the molecular interactions between the two fluids and the solid must be studied, and this region matched to an outer region, where the Navier–Stokes equations would apply. Such an analysis would be very difficult, but it has been suggested that the likely outcome would be equivalent to replacing the no-slip boundary condition by a slip condition, and continuing to employ the Navier–Stokes equations. Such a prescription would not give anything like a complete analysis of the flow, but it might be sufficient to determine such overall features as the total stress sustained by the solid boundary. A similar method has been used in rarefied gas flow, but there the procedure can be justified to some extent, and the slip coefficient quantified. No such justification appears possible in the problem of a moving contact line, and the postulated slip coefficient has no rational basis; all that can be said is that it would have to be of molecular size (the slip coefficient has the dimensions of length).

An alternative approach was presented in part 1 (Hocking 1976). The solid boundary, which has been assumed to be a geometrical plane, is in reality subject to surface irregularities. These dips and hollows are usually on a scale considerably larger than the molecular scale, and part 1 showed that it was possible to model the effect of these surface irregularities by replacing the real surface by a geometrical plane and imposing a slip boundary condition. The essential point is that the displaced fluid continues to occupy the hollows on the surface, so that the displacing fluid is moving over a partly fluid surface. Moreover, for particularly simple corrugated surfaces, an effective slip coefficient was calculated, its size being related in a complicated manner to the dimensions of the hollows as well as to the viscosities of the two fluids.

Although the replacement of the usual no-slip boundary condition by a slip condition, whether for non-continuum reasons or because of surface irregularities, does not have a rational basis, studying a problem involving a moving contact line under this condition would seem to be justified. There is no suggestion, of course, that the slip condition is relevant to all circumstances. The size of the coefficient is sufficient to imply that it can be ignored except in circumstances where the no-slip condition predicts unbounded stresses. In other words, we have a standard singular perturbation problem. For the outer solution, at distances from the contact line large compared with the slip coefficient, the governing equations are the Navier–Stokes equation and the no-slip condition. For the inner solution, at distances from the contact line comparable to the slip coefficient, the slip boundary condition must be applied. The matching of the inner and outer solutions will then yield an expression for the force on the solid boundary produced by the passage of the two fluids along it. As will be shown later, this force is finite, but with a logarithmic dependence on the slip coefficient. Although the slip coefficient based on molecular effects might be three orders of magnitude smaller than one based on surface irregularities, the additional contribution to the force from the motion near the contact line would be increased by only a factor of seven. Also, this part of the force might only be a small fraction of the total force on the boundary produced by the motion of the fluids on parts of the boundary far from the contact line, so that experimental discrimination between the two possible types of slip coefficient would not be straightforward.

The inner problem is formulated with some generality in §2, and particular cases are examined in §§3 and 4. The matching between inner and outer solutions is described in §5, and the outer solutions are then found for flow between parallel planes in §6 and for flow in a pipe in §7.

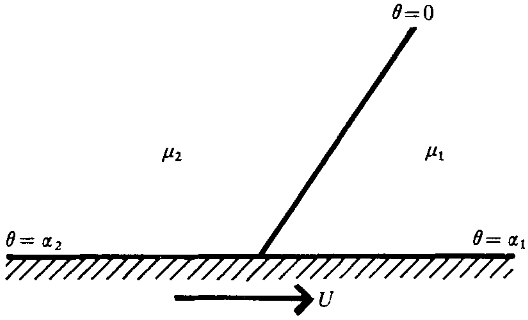

FIGURE 1. Definition sketch for the flow perpendicular to the contact line C.

2. The inner region

The motion in the vicinity of the contact line between the fluid interface and the solid boundary is analysed here under the following assumptions. The scale of the region where slip is important, measured by the size of the slip coefficient, is small compared with the other length scales of the flow; in particular, this implies that the boundary is locally plane. The Reynolds number based on this small length scale is small enough for the Stokes equations to be used. The interface is plane and is moving with constant speed U in a direction perpendicular to its line of contact with the solid boundary, so that the flow is locally two-dimensional.

It is convenient to use a co-ordinate frame moving with the interface. Polar co-ordinates (r, θ) in the plane of the motion are defined such that the origin is on the contact line and the interface is in the plane $\theta = 0$. The sector $0 < \theta < \alpha_1$ is occupied by fluid of viscosity μ_1 and the motion there is given by the stream function $\Psi_1(r, \theta)$; the other fluid, for which the stream function is $\Psi_2(r, \theta)$ and which has viscosity μ_2, occupies the sector $0 > \theta > \alpha_2$, where $\alpha_2 = \alpha_1 - \pi$. The two parts of the plane solid boundary on either side of the contact line are given by $\theta = \alpha_1$ and $\theta = \alpha_2$ (see figure 1). The stream functions satisfy the biharmonic equation

$$\left[\frac{\partial^2}{\partial r^2} + \frac{\partial}{r\,\partial r} + \frac{\partial^2}{r^2\,\partial\theta^2}\right]^2 \Psi = 0, \tag{2.1}$$

and the boundary conditions are

$$\Psi_1(r, 0) = \Psi_1(r, \alpha_1) = \Psi_2(r, 0) = \Psi_2(r, \alpha_2) = 0, \tag{2.2}$$

$$\partial\Psi_1(r, 0)/\partial\theta = \partial\Psi_2(r, 0)/\partial\theta, \quad \mu_1\,\partial^2\Psi_1(r, 0)/\partial\theta^2 = \mu_2\,\partial^2\Psi_2(r, 0)/\partial\theta^2, \tag{2.3}$$

$$\frac{\partial\Psi_1(r, \alpha_1)}{r\,\partial\theta} + \frac{c_1\,\partial^2\Psi_1(r, \alpha_1)}{r^2\,\partial\theta^2} = U, \tag{2.4a}$$

$$\frac{\partial\Psi_2(r, \alpha_2)}{r\,\partial\theta} - \frac{c_2\,\partial^2\Psi_2(r, \alpha_2)}{r^2\,\partial\theta^2} = -U. \tag{2.4b}$$

Conditions (2.2) ensure that the solid boundary and the interface are streamlines, and (2.3) represents continuity of velocity and tangential stress across the interface. The slip conditions at the solid boundary are given by (2.4) and c_1 and c_2 are the slip coefficients for the two fluid–solid contacts. The assumption that the interface is plane is equivalent to the presence of a surface tension between the two fluids which is sufficiently large to accommodate the normal-stress imbalance across the interface with a negligibly small curvature (see the discussion on the validity of this assumption in Huh & Scriven (1971) and in part 1).

With $c_1 = c_2 = 0$, the solution of these equations has the simple similarity form

$$\Psi_1 = Ur\hat{\phi}_1(\theta), \quad \Psi_2 = Ur\hat{\phi}_2(\theta), \tag{2.5}$$

with

$$\hat{\phi}_i(\theta) = a_i\theta\sin(\theta-\alpha_i) + b_i(\theta-\alpha_i)\sin\theta, \quad i = 1, 2. \tag{2.6}$$

Conditions (2.2) are satisfied by this choice of solution, and the remaining conditions determine the four coefficients in (2.6). Equivalent expressions were obtained by Huh & Scriven (1971), who presented a number of examples of streamline patterns. The tangential stresses on the boundary, in a direction opposing the motion of the boundary, are given by

$$\tau_1 = \mu_1 Ur^{-1}\hat{k}_1, \quad \tau_2 = \mu_2 Ur^{-1}\hat{k}_2, \tag{2.7}$$

where

$$\left.\begin{aligned} D\hat{k}_1 &= 2\mu_1\sin^2\alpha_1(\sin^2\alpha_2 - \alpha_2^2) - 2\mu_2\sin^2\alpha_1(\sin^2\alpha_2 - \alpha_1\alpha_2), \\ D\hat{k}_2 &= 2\mu_2\sin^2\alpha_2(\sin^2\alpha_1 - \alpha_1^2) - 2\mu_1\sin^2\alpha_2(\sin^2\alpha_1 - \alpha_1\alpha_2), \end{aligned}\right\} \tag{2.8}$$

and

$$D = \mu_2(\sin\alpha_2\cos\alpha_2 - \alpha_2)(\sin^2\alpha_1 - \alpha_1^2) - \mu_1(\sin\alpha_1\cos\alpha_1 - \alpha_1)(\sin^2\alpha_2 - \alpha_2^2). \tag{2.9}$$

These stresses have a singularity at $r = 0$, and the force on the boundary, if deduced from them, would be infinite.

The similarity solution just obtained has a two-fold importance when an attempt is made to remove the singularity at the origin by means of a slip coefficient. It represents the behaviour of the outer flow in the region of the contact line. Any possible eigensolution proportional to r^λ, say, need not be considered, since if $\lambda > 1$ the forced solution dominates the eigensolution as $r \to 0$, while solutions with $\lambda < 1$ are inadmissible because they give a singular velocity as $r \to 0$. The similarity solution also gives the outer boundary condition for the inner flow.

To determine the flow when the slip conditions (2.4) are applied, we can write

$$\Psi_1 = Ur\phi_1(\rho, \theta), \quad \Psi_2 = Ur\phi_2(\rho, \theta), \tag{2.10}$$

where

$$\rho = \ln(r/c_2), \tag{2.11}$$

and ϕ_1 and ϕ_2 satisfy the new form of (2.1),

$$\left[\left(\frac{\partial}{\partial\rho}+1\right)^2 + \frac{\partial^2}{\partial\theta^2}\right]\left[\left(\frac{\partial}{\partial\rho}-1\right)^2 + \frac{\partial^2}{\partial\theta^2}\right]\phi = 0. \tag{2.12}$$

The boundary conditions (2.2) and (2.3) are unaltered in form, with ϕ_1 and ϕ_2 replacing Ψ_1 and Ψ_2, but the slip conditions (2.4) become

$$\left.\begin{aligned}\frac{\partial\phi_1(\rho,\alpha_1)}{\partial\theta}+\tilde{c}\,e^{-\rho}\frac{\partial^2\phi_1(\rho,\alpha_1)}{\partial\theta^2} &= 1,\\ \frac{\partial\phi_2(\rho,\alpha_2)}{\partial\theta}-e^{-\rho}\frac{\partial^2\phi_2(\rho,\alpha_2)}{\partial\theta^2} &= -1,\end{aligned}\right\} \tag{2.13}$$

where $\tilde{c} = c_1/c_2$. In order that the inner solution should match with the outer solution we must have

$$\phi_1(\infty,\theta) = \hat{\phi}_1(\theta), \quad \phi_2(\infty,\theta) = \hat{\phi}_2(\theta), \tag{2.14}$$

where $\hat{\phi}_1$ and $\hat{\phi}_2$ are given by (2.6), and to ensure that the stress is finite at the origin we must have

$$\phi_1(\rho,\theta) = O(e^{\rho}), \quad \phi_2(\rho,\theta) = O(e^{\rho}) \quad \text{as} \quad \rho\to-\infty. \tag{2.15}$$

The solution of this set of equations can be formulated as a pair of integral equations for the stresses on the boundary, which are the quantities of chief physical interest. We first introduce a two-sided Laplace transform

$$\tilde{\phi}(s,\theta) = \int_{-\infty}^{\infty} e^{-s\rho}\phi(\rho,\theta)\,d\rho \tag{2.16}$$

(the conditions imposed on ϕ_1 and ϕ_2 as $|\rho|\to\infty$ ensure that their transforms exist for $0 < \mathrm{Re}(s) < 1$). Solutions of the transform of (2.12) which satisfy (2.2) are

$$\phi_j = \frac{1}{2\pi i}\int_{\epsilon-i\infty}^{\epsilon+i\infty} e^{s\rho}\{A_j\sin s\theta\sin(\theta-\alpha_j)+B_j\sin\theta\sin s(\theta-\alpha_j)\}\,ds, \quad j = 1,2, \tag{2.17}$$

where $0 < \epsilon < 1$, and A_1, A_2, B_1 and B_2 are functions of s to be found.

If we write the tangential stresses at the boundary as

$$\tau_1 = \mu_1 Ur^{-1}k_1(\rho), \quad \tau_2 = \mu_2 Ur^{-1}k_2(\rho), \tag{2.18}$$

for the two portions $\theta = \alpha_1$ and $\theta = \alpha_2$ respectively, and if the transforms of k_1 and k_2 are denoted by $\tilde{k}_1$ and $\tilde{k}_2$ respectively, the values of the coefficients in (2.17) and (2.21) can be found in terms of $\tilde{k}_1$ and $\tilde{k}_2$ by using (2.3). The transforms of the boundary values of $\partial\phi_1/\partial\theta$ and $\partial\phi_2/\partial\theta$ can then be determined, also in terms of $\tilde{k}_1$ and $\tilde{k}_2$. The inversions of these transforms can then be written as convolution integrals, and we finally obtain, from the boundary conditions (2.13), the integral equations

$$1-\tilde{c}\,e^{-\rho}k_1(\rho) = \int_{-\infty}^{\infty}\{\mu_1 L(\rho-\rho')+\mu_2 M_2(\rho-\rho')\}\,k_1(\rho')\,d\rho' - \int_{-\infty}^{\infty}\mu_2 N(\rho-\rho']\,k_2(\rho')\,d\rho', \tag{2.19a}$$

$$1-e^{-\rho}k_2(\rho) = \int_{-\infty}^{\infty}\{\mu_2 L(\rho-\rho')+\mu_1 M_1(\rho-\rho')\}\,k_2(\rho')\,d\rho' - \int_{-\infty}^{\infty}\mu_1 N(\rho-\rho')\,k_1(\rho')\,d\rho', \tag{2.19b}$$

where

$$L(\rho) = \frac{1}{2\pi i}\int \frac{e^{s\rho}}{2s\Delta}(\sin 2s\alpha_1 - s\sin 2\alpha_1)(\sin 2s\alpha_2 - s\sin 2\alpha_2)\,ds, \tag{2.20}$$

$$M_1(\rho) = \frac{1}{2\pi i}\int \frac{e^{s\rho}}{2s\Delta}(\cos 2s\alpha_1 - 1 - s^2\cos 2\alpha_1 + s^2)(\cos 2s\alpha_2 - \cos 2\alpha_2)\,ds, \tag{2.21}$$

$$M_2(\rho) = \frac{1}{2\pi i}\int \frac{e^{s\rho}}{2s\Delta}(\cos 2s\alpha_2 - 1 - s^2\cos 2\alpha_2 + s^2)(\cos 2s\alpha_1 - \cos 2\alpha_1)\,ds, \tag{2.22}$$

$$N(\rho) = \frac{1}{2\pi i}\int \frac{e^{s\rho}}{2s\Delta}(\sin s\alpha_1\cos\alpha_1 - s\sin\alpha_1\cos s\alpha_1)(\sin s\alpha_2\cos\alpha_2 - s\sin\alpha_2\cos s\alpha_2)\,ds, \tag{2.23}$$

$$\Delta = \mu_1(\cos 2s\alpha_1 - \cos 2\alpha_1)(\sin 2s\alpha_2 - s\sin 2\alpha_2) - \mu_2(\cos 2s\alpha_2 - \cos 2\alpha_2)(\sin 2s\alpha_1 - s\sin 2\alpha_1), \tag{2.24}$$

and the integrals are taken from $\epsilon - i\infty$ to $\epsilon + i\infty$.

The asymptotic values of k_1 and k_2 as $|\rho| \to \infty$ are given by

$$k_1(\rho) \sim e^{\rho}/\tilde{c}, \quad k_2(\rho) \sim e^{\rho} \quad \text{as} \quad \rho \to -\infty, \tag{2.25}$$

$$k_1(\infty) = \hat{k}_1, \quad k_2(\infty) = \hat{k}_2, \tag{2.26}$$

where $\hat{k}_1$ and $\hat{k}_2$ are given by (2.8). If we write $F_1(r)$ and $F_2(r)$ for the forces on a unit width of the boundary, in the direction opposing the motion of the boundary relative to the interface, we have

$$f_1^i(r) = \int_0^r \tau_1\,dr = \mu_1 U \int_{-\infty}^{\ln(r/c_2)} k_1(\rho)\,d\rho, \tag{2.27a}$$

$$f_2^i(r) = \int_0^r \tau_2\,dr = \mu_2 U \int_{-\infty}^{\ln(r/c_2)} k_2(\rho)\,d\rho, \tag{2.27b}$$

and for large r/c_2 we can write

$$f_1^i(r) = \mu_1 U\{\hat{k}_1 \ln(r/c_2) + h_1 + o(1)\}, \tag{2.28a}$$

$$f_2^i(r) = \mu_2 U\{\hat{k}_2 \ln(r/c_2) + h_2 + o(1)\}. \tag{2.28b}$$

Since $\hat{k}_1$ and $\hat{k}_2$ are known already, the main results to be obtained from the solution of (2.19) are the values of h_1 and h_2.

Although a numerical solution of (2.19) could be obtained for any set of values of the parameters α_1, μ_1/μ_2 and c_1/c_2, it does not seem to be feasible to make any simplification of (2.19) in the general case. There are, however, two special cases for which the coupled integral equations can be reduced to uncoupled equations, and these simpler cases are described in the following two sections.

3. A gas–liquid interface

An important special case of the general class of motions under consideration is when one of the two fluids is a gas. The small viscosity ratio permits the force on the portion of the boundary in contact with the liquid to be calculated by ignoring the motion of the gas. It we set $\mu_2 = 0$ in the analysis of §2 and, without loss of generality, let c_1 and c_2 be equal, we obtain the single equation for the stress k_1 in the form

$$1 - e^{-\rho} k_1(\rho) = \int_{-\infty}^{\infty} L_1(\rho-\rho')\, k_1(\rho')\, d\rho', \tag{3.1}$$

where L_1 is the value of $\mu_1 L$, as defined by (2.20) with $\mu_2 = 0$, and is given by

$$L_1(\rho) = \frac{1}{2\pi i}\int_{\epsilon-i\infty}^{\epsilon+i\infty} e^{s\rho} \frac{\sin 2s\alpha_1 - s\sin 2\alpha_1}{2s(\cos 2s\alpha_1 - \cos 2\alpha_1)}\, ds. \tag{3.2}$$

This integral can be reduced to the simpler form

$$L_1(\rho) = \frac{\pi}{4\alpha_1^2}\int_{\rho}^{\infty} \frac{\sinh \rho_1}{\cosh(\pi\rho_1/\alpha_1) - 1}\, d\rho_1, \tag{3.3}$$

which can then be evaluated in terms of elementary functions if α_1 is a rational fraction of π.

The kernel of the integral equation (3.1) has a logarithmic singularity at $\rho' = \rho$. Before attempting a numerical solution of the equation, it is convenient to remove this singularity by writing the equation in the form

$$1 - e^{-\rho} k_1(\rho) = \int_{-\infty}^{\infty} L_1(\rho-\rho')\{k_1(\rho') - k_1(\rho)\}\, d\rho' + k_1(\rho)\int_{-\infty}^{\infty} L_1(\rho-\rho')\, d\rho'. \tag{3.4}$$

It follows from (3.2) that

$$\int_{-\infty}^{\infty} L_1\, d\rho' = \frac{2\alpha_1 - \sin 2\alpha_1}{2(1-\cos 2\alpha_1)} = \hat{k}_1^{-1}, \tag{3.5}$$

so that (3.4) becomes

$$1 - (e^{-\rho} + \hat{k}_1^{-1})\, k_1(\rho) = \int_{-\infty}^{\infty} L_1(\rho-\rho')\{k_1(\rho') - k_1(\rho)\}\, d\rho'. \tag{3.6}$$

The integral in (3.6) tends to zero as $|\rho| \to \infty$, so that

$$k_1(\rho) \sim e^{\rho} \quad \text{as} \quad \rho \to -\infty, \quad k_1(\infty) = \hat{k}_1, \tag{3.7}$$

in agreement with the general results (2.25) and (2.26). The value of $\hat{k}_1$ in (3.5) agrees with that obtained from (2.8) with $\mu_2 = 0$.

The numerical method used for the solution of (3.6) was to define the unknown function by its values at a set of equally spaced points, in a finite interval from -5 to 5 or from -10 to 10, and to evaluate the integral using the midpoint rule. The resulting set of linear equations for the function values was solved by Gauss–Seidel iteration. Convergence was quite rapid, about 15 iterations being required to reduce the residuals to 10^{-5}. The value of the integral in (2.27*a*) could then be found and the value of the coefficient h_1 in the expression (2.28*a*) for the force on the boundary could be estimated. Some values of $\hat{k}_1$, given by (3.5), and of h_1, determined by the above numerical procedure, are given in table 1 for various values of the contact angle α_1,

A check on the numerical method is possible for $\alpha_1 = \frac{1}{2}\pi$, when the integral equation (3.6) has the form

$$1 - (e^{-\rho} + \tfrac{1}{4}\pi)\, k_1(\rho) = \int_{-\infty}^{\infty} \frac{1}{2\pi} \ln\left|\frac{e^{\rho'} + e^{\rho}}{e^{\rho'} - e^{\rho}}\right| \{k_1(\rho') - k_1(\rho)\}\, d\rho'. \tag{3.8}$$

α_1/π	$\hat{k}_1$	h_1
0·05	19·04	−56·33
0·1	9·424	−21·55
0·2	4·522	−7·416
0·25	3·504	−4·334
0·5	1·273	−0·1476
0·75	0·3501	0·6944
0·8	0·2312	0·8398
0·9	0·0612	0·6300

TABLE 1

An alternative method was used in part 1 to solve this particular case. Cartesian co-ordinates were used, x being measured along the interface and y along the boundary, and the solution was found by means of a Fourier sine transform in y. From the solution obtained in part 1, we can deduce, in the present notation, and with the sine and cosine integrals defined as in Abramowitz & Stegun (1965, p. 231), that

$$k_1(\rho) = \frac{4}{\pi}\int_0^\infty \frac{e^\rho \sin(se^\rho)}{1+2s}\,ds = \frac{2}{\pi}e^\rho\{\mathrm{Ci}\,(\tfrac{1}{2}e^\rho)\sin(\tfrac{1}{2}e^\rho) - \mathrm{si}\,(\tfrac{1}{2}e^\rho)\cos(\tfrac{1}{2}e^\rho)\}, \tag{3.9}$$

which is, therefore, the solution of (3.8). Moreover, from this analytic solution we can deduce the value of h_1:

$$h_1 = (4/\pi)(\gamma - \ln 2). \tag{3.10}$$

Simple forms for the kernel of (3.4) can be obtained only for special values of α_1. For $\alpha_1 = \frac{1}{4}\pi$, the values of L_1 and $\hat{k}_1$, as given by (3.3) and (3.5) respectively, are

$$L_1 = \frac{1}{2\pi}\left\{\ln\left|\frac{1+e^{-\rho}}{1-e^{-\rho}}\right| - \operatorname{sech}\rho\right\}, \tag{3.11}$$

$$\hat{k}_1 = 4/(\pi-2), \tag{3.12}$$

and for $\alpha_1 = \frac{3}{4}\pi$,

$$L_1 = \frac{1}{2\pi}\left\{\ln\left|\frac{1+e^{-\rho/3}}{1-e^{-\rho/3}}\right| + \tfrac{1}{3}\operatorname{sech}\tfrac{1}{3}\rho\right\}, \tag{3.13}$$

$$\hat{k}_1 = 4/(3\pi+2). \tag{3.14}$$

For values of α_1 close to 0 and to π, approximate values of the kernel can be found. With $\alpha_1 = \pi\beta$ and β small, we have

$$L_1 = \frac{1}{2\pi}\left[\frac{\sinh|\rho|}{\beta\{\exp(|\rho|/\beta)-1\}} - \ln\{1-\exp(-|\rho|/\beta)\}\right], \tag{3.15}$$

$$\hat{k}_1 = 3/(\beta\pi), \tag{3.16}$$

and the first three values in table 1 were calculated using this approximate kernel. Since the kernel is very small except when $|\rho|$ is close to zero, an approximate solution can be obtained by setting the right-hand side of (3.6) equal to zero, thus obtaining

$$k_1(\rho) = (e^{-\rho} + \tfrac{1}{3}\pi\beta)^{-1}, \tag{3.17}$$

and hence, for small α_1,

$$h_1 \sim -\frac{3}{\alpha}\ln\left(\frac{3}{\alpha}\right). \tag{3.18}$$

The values of h_1 obtained by using this formula are identical, to the accuracy given, with the values shown in table 1 for $\alpha_1/\pi = 0{\cdot}05$ and $0{\cdot}1$, while, for $\alpha_1/\pi = 0{\cdot}2$, (3.18) gives $h_1 = -7{\cdot}464$, compared with $h_1 = -7{\cdot}416$ from the numerical solution.

For values of α_1 close to π, we write $\alpha_1 = \pi(1-\beta)$, and the approximate values of L_1 and $\hat{k}_1$ are

$$L_1 = (2\pi)^{-1}[\exp(-\beta|\rho|)/(2\beta) - \ln\{1-\exp(-|\rho|)\}], \tag{3.19}$$

$$\hat{k}_1 = 2\pi\beta^2, \tag{3.20}$$

which were used to calculate the last two entries in table 1. Since the values of h_1 appear to pass through a maximum as α_1 is increased towards π, an estimate of the behaviour of h_1 as α_1 approaches π is desirable, particularly as the slow variation of the kernel makes numerical computation increasingly difficult in this limit.

Although the second term in the kernel (3.19) is logarithmically infinite at $\rho = 0$, whereas the first term is bounded, the second term can be neglected for small β. It is of comparable magnitude to the first term only when

$$|\rho| < \exp(-1/2\beta),$$

and the contribution to the integral in (3.1) from the second term over this range of ρ is

$$O(\beta^{-1}\exp(-1/2\beta)),$$

which is negligible compared with the $O(\beta^{-1})$ contribution from the first term over the whole range of the integral. It is therefore possible to find the asymptotic solution for small β by solving the integral equation

$$1 - e^{-\rho}k_1(\rho) = \int_{-\infty}^{\infty}\frac{1}{4\pi\beta}\exp(-\beta|\rho'-\rho|)\,k_1(\rho')\,d\rho', \tag{3.21}$$

which can be done as follows.

We first take a two-sided Laplace transform, with the constant term in (3.21) replaced by $\exp(-\epsilon|\rho|)$, where ϵ is a small positive constant. The transformed equation is

$$\tilde{k}_1(s+1) + \frac{1}{2\pi(\beta^2 - s^2)}\tilde{k}_1(s) = \frac{1}{s+\epsilon} - \frac{1}{s-\epsilon}. \tag{3.22}$$

Similar functional equations can also be obtained for arbitrary angles α_1. The only other case, however, in which a solution could be found was the special case $\alpha_1 = \frac{1}{2}\pi$, for which the solution was already known.

To obtain the solution of (3.22), we take $\rho < 0$ and examine the poles of $\tilde{k}_1(s)$ in $\mathrm{Re}\, s > 0$. There must not be a pole at $s = \epsilon$, else k_1 would tend to a constant as $\rho \to -\infty$, in contradiction to (3.7), but there are poles at $s = n+\epsilon, n = 1, 2, \ldots$.

When the transform is inverted, these poles contribute to a particular solution for k_1:

$$k_p = e^{\rho} \sum_{m=0}^{\infty} \frac{(e^{\rho}/2\pi)^m(-\beta)!\,\beta!}{(m-\beta)!\,(m+\beta)!}. \tag{3.23}$$

The poles at $s = n \pm \beta$ produce the complementary function, which can be written as

$$k_c = e^{\rho}[AI_{2\beta}\{(2/\pi)^{\frac{1}{2}}e^{\frac{1}{2}\rho}\} + BI_{-2\beta}\{(2/\pi)^{\frac{1}{2}}e^{\frac{1}{2}\rho}\}], \tag{3.24}$$

where A and B are constants, but we can immediately set $B = 0$, since otherwise the stress would be singular as $\rho \to -\infty$. If we introduce a new variable x, defined by

$$x = (2/\pi)^{\frac{1}{2}}e^{\frac{1}{2}\rho}, \tag{3.25}$$

we obtain

$$k_1 = k_p + k_c = \tfrac{1}{2}\pi x^2\left[\sum_0^{\infty}\frac{(\frac{1}{2}x)^{2m}(-\beta)!\,\beta!}{(m-\beta)!\,(m+\beta)!} + AI_{2\beta}(x)\right], \tag{3.26}$$

and the arbitrary constant A can be determined by the condition

$$k_1(\infty) = \hat{k}_1 = 2\pi\beta^2. \tag{3.27}$$

It is not difficult to show that

$$k_1 = 2\pi\beta^2x^2[K_{2\beta}(x)\int_0^x x_1^{-1}I_{2\beta}(x_1)\,dx_1 + I_{2\beta}(x)\int_x^{\infty} x_1^{-1}K_{2\beta}(x_1)\,dx_1], \tag{3.28}$$

which is the required solution of (3.21). The force on the boundary can then be found, and, making use of standard properties of the Bessel functions, we obtain the asymptotic form of h_1 as $\alpha_1 \to \pi$:

$$h_1 \sim 2(\pi-\alpha_1) - (2/\pi)(\ln(2\pi) - 2\gamma)(\pi-\alpha_1)^2. \tag{3.29}$$

The decreasing values of h_1 at the end of table 1 are confirmed and we have also shown that $h_1 \to 0$ as $\alpha_1 \to \pi$. For $\alpha_1 = 0{\cdot}9\pi$, the value of h_1 given by (3.29) is 0·5854, whereas the calculated value given in table 1 is 0·6300.

For values of α_1 which are not close enough to either 0 or π for these approximate kernels to be used, the kernel must first be determined by the evaluation of (3.3). This can be done explicitly if α_1/π is a simple fraction, but, in general, the numerical procedure would be complicated by the necessity for a numerical evaluation of the kernel.

4. Normal contact

A second case in which the integral equations of §2 can be uncoupled is when the interface has a contact angle of $\frac{1}{2}\pi$ and when, in addition, the slip coefficients c_1 and c_2 are equal. With $\alpha_1 = \frac{1}{2}\pi$ and $\alpha_2 = -\frac{1}{2}\pi$, the integral equations (2.19) can be written as

$$1 - e^{-\rho}k_1(\rho) = \int_{-\infty}^{\infty} P(\rho-\rho')\,k_1(\rho')\,d\rho' - \frac{\mu_2}{\mu_1+\mu_2}\int_{-\infty}^{\infty} Q(\rho-\rho')\{k_1(\rho') + k_2(\rho')\}\,d\rho', \tag{4.1a}$$

$$1 - e^{-\rho}k_2(\rho) = \int_{-\infty}^{\infty} P(\rho-\rho')\,k_2(\rho')\,d\rho' - \frac{\mu_1}{\mu_1+\mu_2}\int_{-\infty}^{\infty} Q(\rho-\rho')\{k_1(\rho') + k_2(\rho')\}\,d\rho', \tag{4.1b}$$

where
$$P(\rho) = \frac{1}{2\pi i}\int_{\epsilon-i\infty}^{\epsilon+i\infty} (2s)^{-1} e^{s\rho} \tan \tfrac{1}{2}\pi s \, ds = \frac{1}{2\pi} \ln \left| \frac{1+e^{-|\rho|}}{1-e^{-|\rho|}} \right|, \tag{4.2}$$

$$Q(\rho) = \frac{1}{2\pi i}\int_{\epsilon-i\infty}^{\epsilon+i\infty} \frac{s\, e^{s\rho}}{\sin \pi s} ds = \frac{1}{2\pi(\cosh\rho+1)}. \tag{4.3}$$

If we write
$$\mu_1 k_1 - \mu_2 k_2 = (\mu_1 - \mu_2) k_a, \quad k_1 + k_2 = 2k_b, \tag{4.4}$$

the integral equations uncouple and become

$$1 - e^{-\rho} k_a(\rho) = \int_{-\infty}^{\infty} P(\rho-\rho') k_a(\rho') \, d\rho', \tag{4.5}$$

$$1 - e^{-\rho} k_b(\rho) = \int_{-\infty}^{\infty} \{P(\rho-\rho') - Q(\rho-\rho')\} k_b(\rho') \, d\rho'. \tag{4.6}$$

The first of these equations is identical with the equation obtained in §3 for a gas–liquid interface with a contact angle of $\frac{1}{2}\pi$, and its exact solution was given there [see (3.8) and (3.9)]. The second equation can be written as

$$1 - \left(\frac{\pi^2-4}{4\pi} + e^{-\rho}\right) k_b(\rho) = \int_{-\infty}^{\infty} \{P(\rho-\rho') - Q(\rho-\rho')\}\{k_b(\rho') - k_b(\rho)\} \, d\rho', \tag{4.7}$$

and a numerical solution can be obtained by the method described in §3.

To find the forces on the two parts of the boundary, we first evaluate the integrals of k_a and k_b. Extending the notation introduced in (2.28), we write

$$\int_{-\infty}^{\ln(r/c)} k_{a,b}(\rho) \, d\rho = \hat{k}_{a,b} \ln(r/c) + h_{a,b}, \tag{4.8}$$

where c is the slip coefficient. From the solution of (4.5) already obtained in §3, we have
$$\hat{k}_a = 4/\pi = 1{\cdot}273, \quad h_a = (4/\pi)(\gamma - \ln 2) = -0{\cdot}1476. \tag{4.9}$$

The values of h_b and $\hat{k}_b$ can be found from the numerical solution of (4.7) and from the asymptotic value of $k_b(\rho)$ as $\rho \to \infty$, and we find

$$\hat{k}_b = 4\pi/(\pi^2 - 4) = 2{\cdot}141, \quad h_b = -1{\cdot}539. \tag{4.10}$$

The values of the coefficients in the expressions (2.28) for the forces on the boundary are then given by applying relations (4.5), so that we obtain

$$\hat{k}_1 = \frac{(\mu_1-\mu_2)\hat{k}_a + 2\mu_2 \hat{k}_b}{\mu_1+\mu_2}, \quad h_1 = \frac{(\mu_1-\mu_2) h_a + 2\mu_2 h_b}{\mu_1+\mu_2}, \tag{4.11a}$$

$$\hat{k}_2 = \frac{-(\mu_1-\mu_2)\hat{k}_a + 2\mu_1 \hat{k}_b}{\mu_1+\mu_2}, \quad h_2 = \frac{-(\mu_1-\mu_2) h_a + 2\mu_2 h_b}{\mu_1+\mu_2}. \tag{4.11b}$$

For a water–air interface, with the viscosity ratio $\mu_1/\mu_2 = 100$, say, we have

$$\hat{k}_1 = 1{\cdot}290, \quad h_1 = -0{\cdot}1752, \tag{4.12a}$$

$$\hat{k}_2 = 2{\cdot}992, \quad h_2 = -2{\cdot}903. \tag{4.12b}$$

In these results, the motion of the air is not neglected. The corresponding results for the part of the boundary in contact with the water when the air motion is neglected were found in §3 and are given by (4.9). The large change in the value of h_1 is due to the value of h_b being an order of magnitude larger than h_a.

5. The outer region

The equations governing the outer region are the Navier–Stokes equations, together with the no-slip boundary condition. For two-dimensional motion, either plane or axisymmetric, the contact line is perpendicular to the flow plane, and the similarity solution (2.10) holds as the contact line is approached. The stresses on the boundary near the contact line have the asymptotic form

$$\tau_1 \sim \mu_1 U\hat{k}_1/r, \quad \tau_2 \sim \mu_2 U\hat{k}_2/r, \tag{5.1}$$

where r is measured along the wall from the contact line. The force per unit length of the contact line on a section of the boundary from $r = r_m$ to $r = R$, where r_m is small compared with the length scale a of the outer region but large compared with the slip coefficient, can be written as

$$f_1^o = \mu_1 U[\hat{k}_1 \ln(a/r_m) + H_1(r_m, R)], \tag{5.2a}$$

$$f_2^o = \mu_2 U[\hat{k}_2 \ln(a/r_m) + H_2(r_m, R)], \tag{5.2b}$$

where H_1 and H_2 are regular as $r_m \to 0$. If we now add the contribution to the force from the inner region, from $r = 0$ to $r = r_m$, as given by (2.28), we obtain for the leading terms of the total force on the boundary

$$F_1 = f_1^o + f_1^i = \mu_1 U[\hat{k}_1 \ln(a/c_2) + h_1 + H_1(0, R)], \tag{5.3a}$$

$$F_2 = f_2^o + f_2^i = \mu_2 U[\hat{k}_2 \ln(a/c_2) + h_2 + H_2(0, R)]. \tag{5.3b}$$

Problems involving two fluids with an interface are not easy to solve, even when the overall Reynolds number is small. One example which can be solved is that of two fluids between parallel plates or in a pipe, with the interface spanning the cross-section. Solutions of these problems have been obtained by Bataille (1966) and by Bhattacharji & Savic (1965), but only with the added restrictions that the interface remains plane and that the dynamics of the fluid on one side of the interface can be neglected, as for a liquid–gas interface. Parallel-plate flow, under these restrictions, but with a slip coefficient, was examined in part 1, and the force on the bounding plates was obtained. The extension of this result to fluids of arbitrary viscosity, but with the contact angle still equal to $\frac{1}{2}\pi$, is the subject of §6, and the corresponding results for pipe flow are in §7. Since the values of $\hat{k}_1$, $\hat{k}_2$, h_1 and h_2 for a contact angle of $\frac{1}{2}\pi$ are given in §4, all that is needed to evaluate the force on the boundary are the values of H_1 and H_2 and the velocity U of the interface.

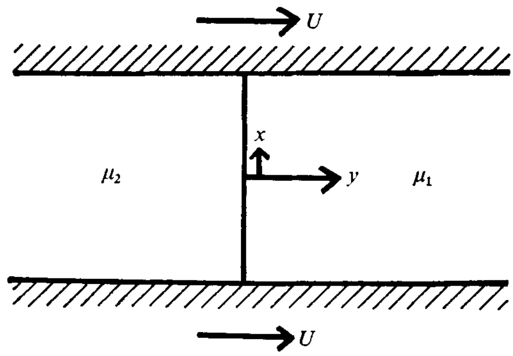

FIGURE 2. A plane interface between parallel plates (§ 6) or in a pipe (§ 7).

6. Parallel-plate flow

The two-dimensional, low Reynolds number flow of two fluids between parallel plates can be formulated as follows. Non-dimensional Cartesian co-ordinates x and y are used, where x is measured normal to the plates and y parallel to them, as shown in figure 2. The half-width a of the gap between the plates is the unit of length, so that the plates are given by $x = \pm 1$, and the plane interface is at $y = 0$. The reference frame moves with the interface, so that the plates have velocity U relative to the interface in the $+y$ direction. The viscosity of the fluid in $y > 0$ is μ_1 and the stream function there is Ψ_1, and μ_2 and Ψ_2 are the corresponding quantities in the region $y < 0$. Both stream functions satisfy the biharmonic equation

$$\nabla^4\Psi = [\partial^2/\partial x^2 + \partial^2/\partial y^2]^2\,\Psi = 0, \tag{6.1}$$

and the boundary conditions

$$\Psi = 0, \quad \partial\Psi/\partial x = -U \quad \text{at} \quad x = \pm 1. \tag{6.2}$$

The matching conditions at the interface $y = 0$ are

$$\Psi_1 = \Psi_2 = 0, \quad \partial\Psi_1/\partial y = \partial\Psi_2/\partial y, \quad \mu_1\,\partial^2\Psi_1/\partial y^2 = \mu_2\,\partial^2\Psi_2/\partial y^2. \tag{6.3}$$

The asymptotic values of the stream functions as $|y| \to \infty$ are

$$\Psi_1, \Psi_2 \sim \tfrac{1}{2}U(x - x^3). \tag{6.4}$$

In a frame at rest relative to the plates, both fluids have the usual parabolic velocity profile at large distance from the interface, with a mean velocity equal to U.

The problem can be split into two subsidiary problems in terms of two new functions, which are respectively odd and even in y. We write

$$\Psi_1 = \tfrac{1}{2}U(x - x^3) + \frac{\mu_1 - \mu_2}{\mu_1 + \mu_2}\,U\phi(x, y) + \frac{2\mu_2}{\mu_1 + \mu_2}\,U\chi(x, y), \tag{6.5a}$$

$$\Psi_2 = \tfrac{1}{2}U(x - x^3) - \frac{\mu_1 - \mu_2}{\mu_1 + \mu_2}\,U\phi(x, -y) + \frac{2\mu_1}{\mu_1 + \mu_2}\,U\chi(x, -y). \tag{6.5b}$$

The odd function ϕ is defined in $y \geqslant 0$ by

$$\left.\begin{aligned} &\nabla^4\phi = 0, \\ &\phi(\pm 1, y) = \partial\phi(\pm 1, y)/\partial x = 0, \\ &\phi(x, 0+) = \tfrac{1}{2}(x^3 - x), \quad \partial^2\phi(x, 0+)/\partial y^2 = 0, \\ &\phi(x, \infty) = 0, \end{aligned}\right\} \tag{6.6}$$

and the even function χ is defined in $y \geqslant 0$ by

$$\left.\begin{aligned} &\nabla^4\chi = 0, \\ &\chi(\pm 1, y) = \partial\chi(\pm 1, y)/\partial x = 0, \\ &\chi(x, 0+) = \tfrac{1}{2}(x^3 - x), \quad \partial\chi(x, 0+)/\partial y = 0, \\ &\chi(x, \infty) = 0. \end{aligned}\right\} \tag{6.7}$$

The value of ϕ can be found by taking a Fourier sine transform

$$\bar{\phi} = \int_0^\infty \sin sy\, \phi(x, y)\, dy, \tag{6.8}$$

and the solution is

$$\phi = \frac{2}{\pi}\int_0^\infty \sin sy \left[\frac{x^3 - x}{2s} - \frac{x \sinh s \cosh sx - \cosh s \sinh sx}{s(\sinh s \cosh s - s)}\right] ds. \tag{6.9}$$

To evaluate the stress on the boundary $x = 1$ we need to find $\partial^2\phi/\partial x^2$ there, and from (6.9) we have

$$\left.\frac{\partial^2\phi}{\partial x^2}\right|_{x=1} = \frac{1}{\pi i}\int_{-\infty}^\infty \frac{e^{isy}}{s}\left(3 - \frac{2s \sinh^2 s}{\sinh s \cosh s - s}\right) ds. \tag{6.10}$$

There is no pole at $s = 0$, and the other poles in the upper half-plane are at $s = is_n, i\bar{s}_n$ (the bar denotes a complex conjugate), where s_n has positive real and imaginary parts,

$$\sin 2s_n = 2s_n, \tag{6.11}$$

and for large n

$$s_n \sim (n + \tfrac{1}{4})\pi + \tfrac{1}{2}i \ln\{(4n+1)\pi\}. \tag{6.12}$$

The integral in (6.10) can be evaluated by summing the residues at the poles in the upper half-plane, and we have

$$\left.\frac{\partial^2\phi}{\partial x^2}\right|_{x=1} = -2\sum_{n=1}^\infty [\exp(-s_n y) + \exp(-\bar{s}_n y)]. \tag{6.13}$$

If the series is integrated from $y = y_0$ to $y = \infty$, and we then let $y_0 \to 0$, the series diverges. To avoid this singularity, we write

$$\int_{y_0}^\infty \left(\left.\frac{\partial^2\phi}{\partial x^2}\right|_{x=1} + \sum_{n=1}^\infty 4\exp(-n\pi y)\right) dy = \sum_{n=1}^\infty \left(\frac{4}{n\pi}\exp(-n\pi y_0) - \frac{2}{s_n}\exp(-s_n y_0) - \frac{2}{\bar{s}_n}\exp(-\bar{s}_n y_0)\right), \tag{6.14}$$

from which we obtain

$$\lim_{y_0\to 0}\left\{\int_{y_0}^{\infty}\frac{\partial^2\phi}{\partial x^2}\bigg|_{x=1}+\frac{4}{\pi}\ln(1/\pi y_0)\right\}=\sum_{n=1}^{\infty}\left(\frac{4}{n\pi}-\frac{2}{s_n}-\frac{2}{\bar{s}_n}\right). \tag{6.15}$$

The asymptotic value of s_n, given in (6.12), shows that the series converges, and the sum was found numerically after the roots of (6.11) had been determined by Newton iteration, with the asymptotic values as initial approximations to the roots. The contribution of the odd part of the complete solution to the force on the boundary can be found by adding to (6.15) the appropriate result for the inner region, given by (4.9), with $r = ay_0$. The force per unit length of the contact line in the direction opposite to the motion of the plates is

$$F_\phi = U\mu_1\left(\frac{4}{\pi}\ln\left(\frac{a}{c}\right)-2{\cdot}18\right). \tag{6.16}$$

Since ϕ decreases more rapidly than e^{-3y} as $y\to\infty$, this result will also hold for a finite length of the plate, unless this length is less than the gap between the plates.

The solution of (6.7) is not so straightforward. A cosine transform,

$$\bar{\chi}=\int_0^\infty \cos sy\,\chi(x,y)\,dy, \tag{6.17}$$

gives the equation

$$\left\{\frac{d^4}{dx^4}-2s^2\frac{d^2}{dx^2}+s^4\right\}\bar{\chi}=\left(\frac{\partial^3\chi}{\partial y^3}\right)_{y=0}=S(x), \tag{6.18}$$

and the solution can be written as an integral by variation of parameters. After a considerable amount of manipulation, and when the transform has been inverted, we obtain

$$\chi=\sum_{n=1}^{\infty}\tfrac{1}{2}\exp(-s_n y)\,U_n(x)\int_0^1 S(x')\,U_n(x')\,dx'+\text{complex conjugate (c.c.)}, \tag{6.19}$$

where

$$U_n(x)=\frac{\cos s_n\sin s_n x - x\cos s_n x\sin s_n}{s_n\sin^4 s_n}, \tag{6.20}$$

and s_n is a root of (6.11). The boundary condition on $y = 0$ can now be used, and we end with an integral equation for S:

$$\sum_{n=1}^{\infty}U_n(x)\int_0^1 S(x')\,U_n(x')\,dx'+\text{c.c.}=x^3-x. \tag{6.21}$$

The stress on the boundary can then be found in terms of S, since we have

$$\frac{\partial^2\chi}{\partial x^2}\bigg|_{x=1}=\sum_{n=1}^{\infty}\exp(-s_n y)\int_0^1 S(x')\,U_n(x')\,dx'+\text{c.c.} \tag{6.22}$$

Although this appears to be the most satisfactory form of the problem, the numerical solution of (6.22) did not prove to be straightforward. An alternative method is to note from (6.19) that the solution can be expressed in the form

$$\chi=\tfrac{1}{2}\sum_{n=1}^{\infty}\exp(-s_n y)\,a_n s_n U_n(x)+\text{c.c.}, \tag{6.23}$$

so that $\{U_n(x)\}$ forms a complete set of eigensolutions for the problem, satisfying the four conditions at $x = \pm 1$. The boundary conditions on $y = 0$ give

$$\tfrac{1}{2}\sum_{n=1}^{\infty} a_n s_n U_n(x) + \text{c.c.} = \tfrac{1}{2}(x^3 - x), \tag{6.24a}$$

$$\tfrac{1}{2}\sum_{n=1}^{\infty} a_n s_n^2 U_n(x) + \text{c.c.} = 0, \tag{6.24b}$$

and if we multiply these equations by $\sin m\pi x$ (m being a positive integer) and integrate from -1 to $+1$, we obtain two infinite sets of equations for the coefficients:

$$\sum_{n=1}^{\infty} \frac{s_n a_n}{(s_n^2 - m^2\pi^2)^2} + \text{c.c.} = \frac{3}{(m\pi)^4}, \tag{6.25a}$$

$$\sum_{n=1}^{\infty} \frac{s_n^2 a_n}{(s_n^2 - m^2\pi^2)^2} + \text{c.c.} = 0. \tag{6.25b}$$

These equations were truncated at $m = n = 50$ and solved. The force on the boundary from $y = y_0$ to $y = \infty$ is proportional to

$$\int_{y_0}^{\infty} \left.\frac{\partial^2 \chi}{\partial x^2}\right|_{x=1} dy = \sum_{n=1}^{\infty} a_n \exp(-s_n y_0) + \text{c.c.} \tag{6.26}$$

This quantity was evaluated for small values of y_0 and extrapolation to $y_0 = 0$ gave the value

$$\int_{y_0}^{\infty} \left.\frac{\partial^2 \chi}{\partial x^2}\right|_{x=1} dy \sim \frac{4\pi}{\pi^2 - 4} \ln y_0 + 2{\cdot}64. \tag{6.27}$$

Combining this result with the contribution from the inner region, we have, for the force on the boundary corresponding to the even part of the solution,

$$F_\chi = \mu_1 U \left\{\frac{4}{\pi^2 - 4} \ln\left(\frac{a}{c}\right) - 4{\cdot}18\right\}. \tag{6.28}$$

This result, also, will hold for a finite length of the plate unless this length is less than the gap between the plates.

The contribution of the first term of (6.5) to the force is proportional to the length l of pipe, measured from the interface, and we finally have the result that the force per unit length of the contact line on a portion of the plate of length l_1 in contact with the fluid of viscosity μ_1, in the direction of the motion of the interface, is

$$F_1 = \mu_1 U \left[\frac{3l_1}{a} + \frac{\mu_1 - \mu_2}{\mu_1 + \mu_2}\left\{\frac{4}{\pi} \ln\left(\frac{a}{c}\right) - 2{\cdot}18\right\} + \frac{2\mu_2}{\mu_1 + \mu_2}\left\{\frac{4\pi}{\pi^2 - 4} \ln\left(\frac{a}{c}\right) - 4{\cdot}18\right\}\right], \tag{6.29}$$

while the force on a length l_2 of the plate in contact with the fluid of viscosity μ_2 is

$$F_2 = \mu_2 U \left[\frac{3l_2}{a} - \frac{\mu_1 - \mu_2}{\mu_1 + \mu_2}\left\{\frac{4}{\pi} \ln\left(\frac{a}{c}\right) - 2{\cdot}18\right\} + \frac{2\mu_1}{\mu_1 + \mu_2}\left\{\frac{4\pi}{\pi^2 - 4} \ln\left(\frac{a}{c}\right) - 4{\cdot}18\right\}\right]. \tag{6.30}$$

7. Pipe flow

The axisymmetric analogue of the parallel-plate flow of §6 is flow in a pipe of radius a. The configuration is again as sketched in figure 2, which now represents a cross-section through the axis of the pipe, x being measured radially outwards from the axis. The stream functions in the two regions on either side of the interface $y = 0$ satisfy

$$D^4\Psi = \left[\frac{\partial^2}{\partial x^2} - \frac{\partial}{x\,\partial x} + \frac{\partial^2}{\partial y^2}\right]^2 \Psi = 0 \tag{7.1}$$

and the boundary conditions

$$\Psi = 0, \quad x^{-1}\,\partial\Psi/\partial x = -\,U \quad \text{on} \quad x = 1. \tag{7.2}$$

In addition, the velocity must not be singular on the axis. The matching conditions (6.3) at the interface are unchanged. The asymptotic values of the stream functions as $|y| \to \infty$ are now

$$\Psi_1, \Psi_2 \sim \tfrac{1}{2}U(x^2 - x^4). \tag{7.3}$$

Subsidiary functions ϕ and χ can be defined as before, the only alteration to (6.5) being a change in the first term from the value of the stream function at large $|y|$ given by (6.4) to that given by (7.3). The odd function $\phi(x, y)$ is defined by

$$\left.\begin{aligned} D^4\phi &= 0,\\ \phi(1,y) = \partial\phi(1,y)/\partial x = 0, &\quad \phi(0,y) = \partial\phi(0,y)/\partial x = 0,\\ \phi(x,0+) = \tfrac{1}{2}(x^4 - x^2), &\quad \partial^2\phi(x,0+)/\partial y^2 = 0,\\ \phi(x,\infty) &= 0, \end{aligned}\right\} \tag{7.4}$$

and can be found by means of a Fourier sine transform. The solution is

$$\phi = \frac{2}{\pi}\int_0^\infty \sin sy\left[\frac{x^4 - x^2}{2s} + \frac{x^2 I_2(sx)\,I_1(s) - xI_1(sx)\,I_2(s)}{s^2(I_0(s)\,I_2(s) - I_1^2(s))}\right] ds. \tag{7.5}$$

The stress on the boundary $x = 1$, $y > 0$ is

$$\tau_1 = \mu_1 U\left[\frac{\partial}{\partial x}\left(\frac{1}{x}\frac{\partial\phi}{\partial x}\right)\right]_{x=1},$$

and from (7.5) we have

$$\left.\frac{\partial^2\phi}{\partial x^2}\right|_{x=1} = -2\sum_{n=1}^{\infty} \exp(-\sigma_n x) + \text{c.c.}, \tag{7.6}$$

where the σ_n are the roots with positive real and imaginary parts of the equation

$$J_0(\sigma)\,J_2(\sigma) - J_1^2(\sigma) = 0, \tag{7.7}$$

and for large n

$$\sigma_n \sim (n + \tfrac{1}{2})\,\pi + \tfrac{1}{2}i\ln\{(4n+1)\pi\}. \tag{7.8}$$

The determination of the force on the boundary and the treatment of the singular part follow the same lines as were explained in §6, and when the contribution from the inner region is added, we have for the force per unit length of the contact line in the direction opposing the motion of the pipe boundary

$$F_\phi = U\mu_1 \left\{\frac{4}{\pi}\ln\left(\frac{a}{c}\right) - 1{\cdot}90\right\}. \tag{7.9}$$

The even part of the solution is defined by

$$\left.\begin{aligned} D^4\chi &= 0, \\ \chi(1,y) = \partial\chi(1,y)/\partial x = 0, \quad \chi(0,y) &= \partial\chi(0,y)/\partial x = 0, \\ \chi(x,0) = \tfrac{1}{2}(x^4 - x^2), \quad \partial\chi(x,0)/\partial y &= 0, \\ \chi(x,\infty) &= 0. \end{aligned}\right\} \tag{7.10}$$

Similar analysis to that used in §6 produces the result

$$\chi = \sum_{n=1}^{\infty} \frac{\exp(-\sigma_n y)}{2\sigma_n} V_n(x) \int_0^1 xS(x') V_n(x')\,dx' + \text{c.c.}, \tag{7.11}$$

where

$$V_n(x) = \frac{xJ_2(\sigma_n x) J_1(\sigma_n) - J_1(\sigma_n x) J_2(\sigma_n)}{J_1^2(\sigma_n)}, \tag{7.12}$$

and the σ_n are the roots of (7.7). Since $\{V_n(x)\}$ thus forms a complete set of eigen-solutions, we can, as in §6, write

$$\chi = \sum_{n=1}^{\infty} \tfrac{1}{2}\exp(-\sigma_n y)\, x b_n V_n(x) + \text{c.c.}, \tag{7.13}$$

and the boundary conditions at $y = 0$ then give

$$\sum_{n=1}^{\infty} b_n x V_n(x) + \text{c.c.} = x^4 - x^2, \tag{7.14a}$$

$$\sum_{n=1}^{\infty} b_n \sigma_n x V_n(x) + \text{c.c.} = 0. \tag{7.14b}$$

These equations can be multiplied by $J_1(j_m x)$, where the j_m ($m = 1, 2, \ldots$) are the positive roots of $J_1(j) = 0$, and integrated from 0 to 1 to give the two infinite sets of equations for the coefficients:

$$\sum_{n=1}^{\infty} \frac{\sigma_n b_n}{(\sigma_n^2 - j_m^2)^2} + \text{c.c.} = \frac{4}{j_m^4}, \tag{7.15a}$$

$$\sum_{n=1}^{\infty} \frac{\sigma_n^2 b_n}{(\sigma_n^2 - j_m^2)^2} + \text{c.c.} = 0. \tag{7.15b}$$

A numerical solution of these equations, and the value of the force on the boundary, can be obtained as described in §6, and when the contribution from the inner region is added, we have for the force on the pipe boundary per unit length of the contact line

$$F_\chi = \mu_1 U\left[\frac{4\pi}{\pi^2 - 4}\ln\left(\frac{a}{c}\right) - 4{\cdot}66\right]. \tag{7.16}$$

c/a	μ_1/μ_2	e_1	e_2
10^{-3}	1	2·53	2·53
	2	2·26	2·80
	10	1·87	3·19
	100	1·74	3·32
10^{-6}	1	6·23	6·23
	2	5·46	7·00
	10	4·34	8·12
	100	3·97	8·49

TABLE 2

Adding the appropriate multiples of F_ϕ and F_χ together, and including the contribution from the flow at large distances from the interface, we have, finally,

$$F_1 = 2\pi a\mu_1 U\left[\frac{4l_1}{a}+\frac{\mu_1-\mu_2}{\mu_1+\mu_2}\left\{\frac{4}{\pi}\ln\left(\frac{a}{c}\right)-1\cdot 90\right\}+\frac{2\mu_2}{\mu_1+\mu_2}\left\{\frac{4\pi}{\pi^2-4}\ln\left(\frac{a}{c}\right)-4\cdot 66\right\}\right] \tag{7.17a}$$

and

$$F_2 = 2\pi a\mu_2 U\left[\frac{4l_2}{a}-\frac{\mu_1-\mu_2}{\mu_1+\mu_2}\left\{\frac{4}{\pi}\ln\left(\frac{a}{c}\right)-1\cdot 90\right\}+\frac{2\mu_1}{\mu_1+\mu_2}\left\{\frac{4\pi}{\pi^2-4}\ln\left(\frac{a}{c}\right)-4\cdot 66\right\}\right] \tag{7.17b}$$

for the forces on lengths l_1 and l_2 of the pipe in contact with the fluids of viscosity μ_1 and μ_2 respectively. These forces are in the direction of motion of the interface.

If we write

$$F_1 = 8\pi\mu_1 U[l_1+e_1 a],\quad F_2 = 8\pi\mu_2 U[l_2+e_2 a], \tag{7.18a, b}$$

e_1 and e_2 measure the effective increases in length of the two sections of the pipe, measured in units of the pipe radius. Values of e_1 and e_2, calculated from (7.17), for four values of the viscosity ratio and two values of the slip coefficient are given in table 2. For a tube of radius 10^{-2} m, the larger value of c/a is of the size expected when the roughness of the pipe wall is of order 10^{-5} m, and the smaller value is closer to the value which might be expected if slip takes place because of events on a molecular length scale.

For the larger value of the slip coefficient, these results indicate that for slugs of fluid of length large compared with the pipe radius the additional contribution to the resistance emanating from the interfaces between the fluids is not significant, although the extra resistance is infinite if there is no slip. Only for the smaller value of the slip coefficient, and for lengths up to 100 radii, is the effect of the interface on the resistance likely to be a measurable quantity. This is perhaps why serious errors have not been introduced when no consideration has been given to the presence of a fluid interface. For pipe flows, the area of contact between solid and fluid is large compared with the cross-sectional area of the pipe, and the contribution to the resistance from the vicinity of the contact line is relatively unimportant. The interface may play a more significant role in flows which do not contain such a large area of contact. An example is the motion of a drop on an inclined plane.

The flow produced by a closely fitting piston in a pipe also has a force singularity, at the contact line between the face of the piston and the pipe wall. Although there is no longer a fluid interface present, the solution can at once be written down from the analysis already presented. If the face of the piston is at $y = 0$ in a frame moving with the piston at speed U, and if the fluid, of viscosity μ_1, is in the region $y > 0$, the stream function satisfies conditions (7.10). Hence the value of the force on a portion of the pipe of length l is, from (7.16),

$$F_p = 2\pi a \mu_1 U \left\{\frac{4l}{a} + \frac{4\pi}{\pi^2 - 4} \ln(a/c) - 4{\cdot}66\right\}. \tag{7.19}$$

If, as before, we write this force as

$$F_p = 8\pi\mu_1 U(l + e_p a), \tag{7.20}$$

the length of the column of fluid is effectively increased by $e_p a$, where

$$e_p = 2{\cdot}53 \quad \text{if} \quad c/a = 10^{-3}, \quad e_p = 6{\cdot}23 \quad \text{if} \quad c/a = 10^{-6}.$$

Numerical solutions of the transition from plug to tube flow in a pipe have been obtained by Wagner (1975). His calculations cover a wide range of Reynolds numbers, and for low Reynolds numbers he finds that, in terms of the axial pressure drop along the tube, the effect of the transition is equivalent to an increase in length of about $1{\cdot}1\,a$, where a is the tube radius. While recognizing that there is a singularity at the contact line, he states that the best results were obtained by treating the corner as a regular wall point. Since he does not calculate the force on the boundary, but only the *axial* pressure drop, his solution avoids the force singularity, and he does not need to calculate the flow in the vicinity of the contact line accurately. The values of e_p calculated here show that Wagner's solution for low Reynolds numbers would not give accurate values of the force needed to move the piston (an exact solution of the problem he poses, and solves numerically, would give an infinite force, since the no-slip condition is applied). For large Reynolds numbers, Wagner's value for the effective increase in length, as determined from the axial pressure drop, is $\frac{1}{32}a\,Re$, where Re is the Reynolds number, and the related extra force required to move the piston is much larger than the force which must be added because of the slip flow near the contact line, given by (7.19), which is independent of the Reynolds number.

These two problems of the displacing of a fluid in a pipe by another fluid or by a solid piston and the expressions (7.17) and (7.19) for the forces on the boundary satisfy the requirement laid down by Dussan V. & Davis (1974) in their discussion of the proposal to remove the singularity in the force at a contact line by a slip coefficient. They state, "It is therefore essential that the solution of posed boundary-value problems containing slip coefficients be able to predict some measurable physical quantities before the imposed slip is taken as a reasonable description of the local boundary condition."

REFERENCES

ABRAMOWITZ, M. & STEGUN, I. A. 1965 *Handbook of Mathematical Functions*. Dover.
BATAILLE, J. 1966 *C. R. Acad. Sci. Paris*, **262**, 843.
BHATTACHARJI, S. & SAVIC, P. 1965 *Proc. Heat Transfer Fluid Mech. Inst.*, p. 248.
DUSSAN V., E. B. & DAVIS, S. H. 1974 *J. Fluid Mech.* **65**, 71.
HOCKING, L. M. 1976 *J. Fluid Mech.* **76**, 801.
HUH, C. & SCRIVEN, L. E. 1971 *J. Colloid Interface Sci.* **35**, 85.
WAGNER, M. H. 1975 *J. Fluid Mech.* **72**, 257.